

Properties of Carbon Nanotubes under External Factors

Yaroslav V. Shtogun and Lilia M. Woods
University of South Florida
USA

1. Introduction

Carbon nanotubes are quasi-one dimensional nanostructures with many unique properties. These materials are considered as promising building blocks in nanoelectronics, spintronics, and nano-electromechanics. Potential applications of carbon nanotubes have strongly relied on their extraordinary ability of property changes upon external factors, such as mechanical alterations or applied external fields. The success in application of carbon nanotubes has significantly depended on predictions from theoretical calculations and modeling. In particular, first principal simulation methods have proven to be useful techniques in predicting the fundamental nature of changes in carbon nanotube properties and how these properties can be altered under external factors. There is a considerable amount of research on simulations of carbon nanotubes under one type of external factors, such as mechanical defects, mechanical deformations, applied external electric fields, *or* applied external magnetic fields. However, the development and design of current and new carbon nanotube based nanodevices has led to the search of additional ways to modify and tailor their properties. To achieve this flexibility, researchers have begun to study the influence of more than one external factor simultaneously. This is a relatively new area which opens up more possibilities for new devices. Thus, the knowledge of physical property changes in carbon nanotubes under several external factors is crucial for fundamental science and technological prospects.

Our primary focus in this chapter is first principal simulations of electronic and magnetic properties of single wall carbon nanotubes under two external factors. The discussion involves understanding the combined effect of radial deformation *and* mechanical defects, such as a Stone-Wales defect, nitrogen impurity, and mono-vacancy in the carbon network. Furthermore, we will discuss the nanotube property changes due to the application of radial deformation *and* external electric field. To provide the basis for further arguments, we start with a review of important results of carbon nanotubes under one external factor such as mechanical deformations, mechanical defects, or external fields. After we provide the description of the calculation method and model, we arrive at the major issue of radially deformed carbon nanotubes with defects or external electric field. We start with the analysis of the structural changes in defective carbon nanotubes under two types of radial deformations. One is deformation achieved by squeezing of the nanotube between two hard

narrow surfaces, which have width smaller than the nanotube cross section. The other one is achieved by squeezing of the nanotube between two hard surfaces with width larger than the nanotube cross section. As a result, we show the characteristic energies of deformation and defect-formation. Further, we show first principal calculations of band gap modulations, band structure evolutions, and changes in magnetic properties of carbon nanotubes in terms of types of defects and degrees of radial deformation. A special consideration is given to the mechanically induced magnetic properties. Finally, we present the combined effect of radial deformation and external electric field on the nanotube electronic structure and band gap modulations. The chapter reveals greater capabilities for carbon nanotube applications in new devices.

2. Carbon Nanotubes under One External Factor

In many earlier theoretical calculations, carbon nanotubes were considered to be with perfect structure, where ideal graphite plane was rolled up into a cylindrical tube. Depending on the particular way of graphene rolling, nanotubes can be metallic or semiconducting. The rolling direction is characterized by a chiral index (n, m) . Achiral zigzag $(n,0)$ and armchair (n,n) nanotubes are distinguished from the rest (chiral nanotubes). Armchair tubes are always metallic, while zigzag tubes can be semiconducting or metallic (Reich et al., 2004). It has been revealed that these nanostructures have interesting mechanical and electronic properties strongly depended on chirality, which immediately drew interest to their application in micro-electro-mechanics, spintronics, and nanoelectronics. However, experimental measurements have shown that the nanotube structure is not perfect (Fan et al., 2005; Hashimoto et al., 2004; Suenaga et al., 2007). External factors, such as mechanical deformations, mechanical defects, or applied external fields can induce various changes in nanotube properties. In addition, researchers have realized that these external factors can be used in new methods to control and/or tune carbon nanotube properties for practical applications.

2.1 Mechanical Deformation of Carbon Nanotubes

Carbon nanotubes have high elastic modulus, strength, flexibility, and low mass density, which makes them excellent candidates for polymer composite materials and nano-devices (Ashraf et al., 2006; Fennimore et al., 2003; Itkis et al., 2008). They are rigid in the axial direction while they are flexible in the radial direction. In actual experiments, nanotubes undergo structural modifications such as bending, twisting, stretching, and radial deformation (Barboza et al., 2008; Cohen-Karni et al., 2006; Falvo et al., 1997). It has been suggested that the most common mechanical deformation is radial squeezing. Such deformation takes place in bundles of nanotubes, under applied hydrostatic pressure, in interaction of nanotubes with surfaces, nano-indentation experiments, and atom force microscopy (AFM) squeezing of nanotubes (Hertel et al., 1998; Minary-Jolandan & Yu 2008; Tang et al., 2000). In many experiments the carbon nanotubes are manipulated by an AFM tip. This has a major effect not only on the mechanical, but also on the electronic and transport properties of nanotubes. For instance, pressing suspended nanotube over trench by an AFM tip causes the local deformation in the nanotube structure (Fig. 1). Subsequently, the deformed region affects the electron flow between the source and drain electrodes, and

as a result, the conductance of carbon nanotubes decreases several times as compared to the theoretically predicted one (Leonard et al., 2005; Maiti et al., 2002).

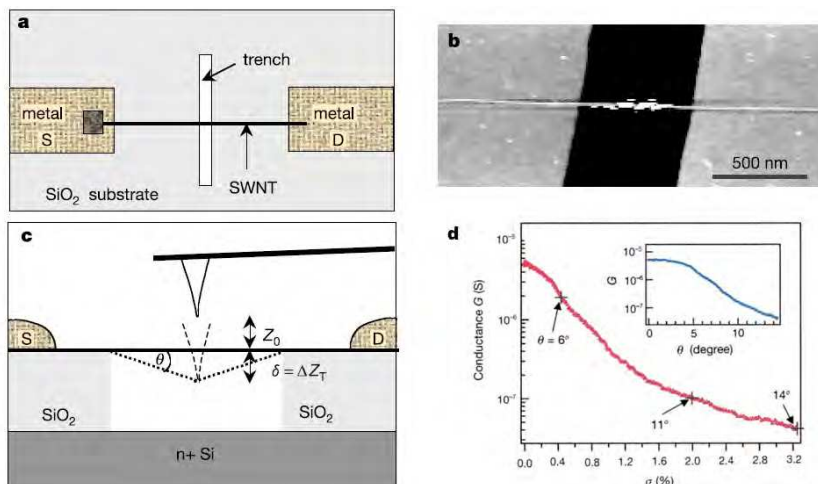


Fig. 1. Electromechanical measurements of a partly suspended nanotube over a trench. a) Device view from above. The substrate has a trench of 500 nm in width and 175 nm in depth. A pair of metal electrodes (S – source and D – drain) is bridged by nanotube suspended over the trench. b) An atom force microscopy image of suspended nanotube. c) Side view of experimental setup when the nanotube is pushed into a trench by atom force microscopy tip. d) Experimentally measured conductance of nanotube as a function of strain. All figures are from (Tomblere et al., 2000).

Cross-sectional changes of carbon nanotube geometry under radial deformation are characterized by two applied strains ϵ_{xx} and ϵ_{yy} along x and y axis, respectively, and they are defined as follows:

$$\epsilon_{xx} = \frac{D_0 - a}{D_0} \tag{1}$$

and

$$\epsilon_{yy} = \frac{D_0 - b}{D_0} \tag{2}$$

where D_0 is the diameter of the undeformed nanotube, a and b are the major and minor axes of the ellipse (Fig. 2a-b). For discussion purposes here we use percentage (%) values of the applied strains ϵ_{xx} and ϵ_{yy} . Depending on the degree of radial deformation, the radial cross section of the nanotube can take a different form. When the applied strain is small, the nanotube has an elliptical-like shape. However, if the applied strain continues to increase, then nanotube cross section undergoes Peanut-like or Flat-like forms. The Peanut-like form corresponds to squeezing of the nanotube between two hard surfaces with a cross section smaller than its radial one, while the Flat-like form corresponds to radial squeezing between two hard surfaces with a cross section larger than its radial one (Fig. 2c-d). The Peanut and Flat deformations can also occur during the experimental measurements when the size of AFM tip is smaller or larger than the cross section of the nanotube.

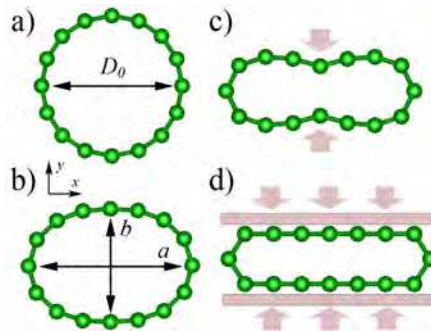


Fig. 2. Cross section view of (8,0) nanotubes under radial deformation. a) Perfect nanotube. b) Nanotube under small radial deformation with elliptical shape of the cross section. c) Peanut-like deformed nanotube. d) Flat-like deformed nanotube.

First principal calculations have shown that the band gap of zigzag semiconductor nanotubes decreases with the increase of radial deformation while for zigzag metallic nanotube it increases and then decreases (Fig. 3). At the same time, if the mirror symmetry of armchair carbon nanotubes is not broken, the radial deformation does not have any effect on the band gap (Gulseren et al., 2002; Park et al., 1999). Therefore, the application of radial deformation causes chirality dependent semiconductor-metal and metal-semiconductor transitions in carbon nanotubes. There are several factors responsible for these transitions, such as σ - π hybridization of the atomic orbitals located on the high curvature regions, interaction between low curvature regions, breaking mirror-symmetry of carbon nanotubes, and geometry deformations (Giusca et al., 2007; Gulseren et al., 2002; Mazzoni & Chacham 2000; Mehrez et al., 2005; Shan et al., 2005; Vitali et al., 2006).

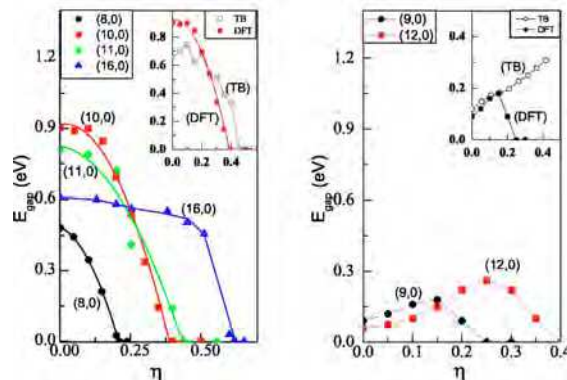


Fig. 3. Density Functional Theory (DFT) calculations of the band gap as a function of the cross sectional flatterness for variety of semiconductor (left panel) and metallic (right panel) carbon nanotubes. The insets on both panels compare tight-binding (TB) and DFT results for (10,0) and (9,0) nanotubes, respectively from (Shan et al., 2005).

2.2 Mechanical Defects in Carbon Nanotubes

The presence of mechanical defects in carbon nanotube structure drastically affects all their properties such as transport, mechanical, magnetic, electronic, and optical. Defects can occur during growth, purification, alignment, or device application processes. They can also be introduced intentionally to modify the carbon nanotube properties. Common defects are Stone-Wales defects (Fig.4b), substitutional impurities (Fig. 4c), and vacancies (Fig. 4d). A Stone-Wales defect takes place in a carbon network when one C-C bond is rotated by 90° degree (Stone & Wales 1986). Such rotation creates two pairs of a pentagon and a heptagon around the rotated C-C bond. It is also known as a 5-7-7-5 defect (Nardelli et al., 2000). The pentagon/heptagon pairs create a local disturbance which serves as a reactive center for adsorption of various atoms, nanoparticles, and molecules (Bettinger 2005; Picozzi et al., 2004; Yang et al., 2006). Increasing the concentration of Stone-Wales defects leads to semiconductor-metal transitions in zigzag nanotubes. It also increases the density of states around the Fermi level for armchair nanotubes due to new defect states, thus, making the tubes more metallic (Crespi & Cohen 1997).

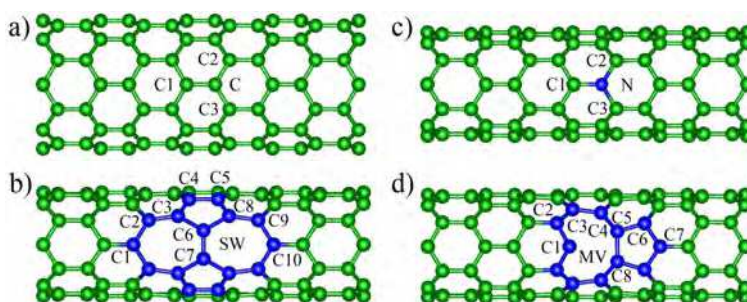


Fig. 4. Side view of (8,0) nanotube structure a) without deformation, and with different defects at $\epsilon_{yy} = 20\%$ deformation for b) a Stone-Wales defect, c) nitrogen substitutional impurity, and d) mono-vacancy. The atoms of the defective sites are labeled.

A substitutional impurity in nanotube can happen when a carbon atom is substituted by a foreign one (Fig. 4c). It has been considered that the common doping atoms in carbon nanotubes are boron and nitrogen, which can appear during laser-ablation and arc-discharge synthesizing processes or during substitutional reaction methods (Droppa et al., 2002; Gai et al., 2004; Golberg et al., 1999). Since B and N atomic radii have similar size to the C atom, they create a small perturbation in the nanotube structure in comparison to the perfect one. However, other atoms such as Li, K, Br, and Ni, which can create a larger disturbance, are also considered for new nano-device application of nanotubes (Lee et al., 1997; Santos et al., 2008). The B and N serve as acceptors and donors of electrons in the nanotubes, respectively, since B has one electron less and N has one electron more than the carbon atom. Theoretical calculations have revealed that such impurities lead to the shift of the Fermi level, additional impurity states in the band structure, and a break of the nanotube mirror symmetry (Czerw et al., 2001; Moradian & Azadi 2006; Yi & Bernholc 1993). Fig. 5b shows evidence of new impurity levels in the density of states of (10,0) nanotube around the Fermi level under nitrogen and boron doping. The impurity effect on electronic properties becomes more evident if their concentration increases. Nitrogen doping has drawn

substantial interest due to the one extra electron provided by a nitrogen atom, which causes magnetic effects in nanotubes, transforms semiconductor nanotube to metallic one, and serves as a reactive center in the interaction of nanotubes with other molecules (Nevidomskyy et al., 2003).

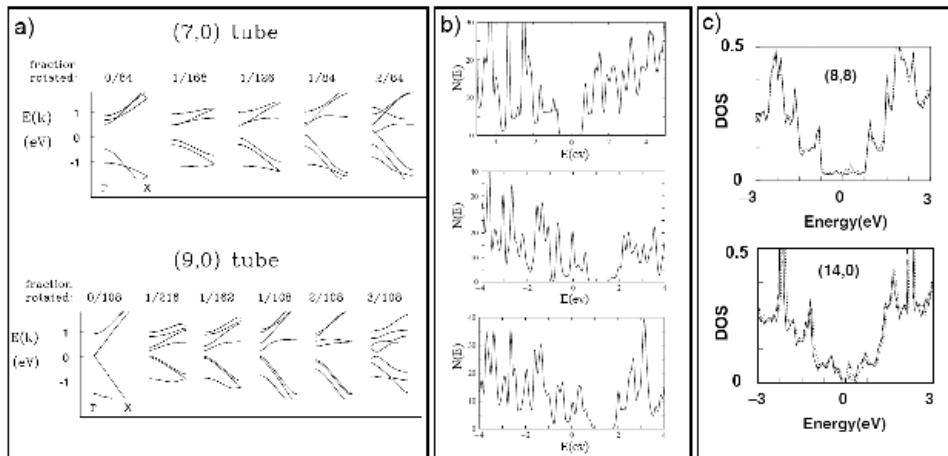


Fig. 5. Band structure and density of states of defective nanotubes. a) Band structure evolutions of (7,0) and (9,0) nanotubes upon increasing the concentration of Stone-Wales defect from (Crespi et al., 1997). b) Density of states (top) of (10,0) nanotube, (middle) where one of carbon atom is substituted by a nitrogen atom, and (bottom) where a carbon atom is substituted by a boron atom in the supercell of 120 carbon atom from (Moradian & Azadi 2006). The nitrogen and boron defect concentration is 0.83%. c) Density of states for (8,8) and (14,0) nanotubes without/with mono-vacancy defect in their structure (solid/dashed line respectively) from (Lu & Pan 2004).

Furthermore, removing a carbon atom leaves a vacancy defect with three dangling carbon bonds in the nanotube network (Rossato et al., 2005). These three dangling bonds are unstable and undergo recombination to make a chemical bond between two of them forming a pentagon ring and one remaining dangling bond – in a nonagon ring (Fig. 4d) (Berber, S. & Oshiyama 2006). The existence of vacancies has been demonstrated experimentally (Hashimoto et al., 2004). It occurs during synthesis of nanotubes or under intentional ion or electron irradiation techniques (Krashennnikov et al., 2001; Krashennnikov et al., 2005). The formation of vacancy and its orientation depends on the radius and chirality of nanotubes. Such a disturbance causes significant changes in their transport, magnetic, mechanical, and optical properties (Orellana & Fuentealba 2006; Tien et al., 2008; Yuan & Liew 2009). Fig. 5c shows the density of state of (8,8) and (14,0) carbon nanotubes without a vacancy (solid line) and with vacancy defect (dashed line). The vacancy defect gives the sharp peak in the density of states above the Fermi level, which consists of localized states from the C dangling bond. Such imperfections can reduce the mean-free path and mobility of the free carrier in nanotubes. This leads to the decrease in the nanotube conductivity. On the other hand, the dangling bond can participate in the interaction with other molecules as well as it can be the center of functionalization of nanotubes. Theoretical

studies have shown that carbon nanotubes with vacancies demonstrate ferromagnetic ordering due to the dangling bond of the nonagon ring (Orellana & Fuentealba 2006). Moreover, the magnetic moment depends on the defect concentration. It opens up opportunities for the application of carbon nanotubes in spintronics, logical, and memory storage devices.

2.3 Carbon Nanotubes under External Fields

The successful application of carbon nanotubes in nano-devices such as field-effect-transistors (Tans et al., 1998), rectifiers (Yao et al., 1999), p-n junctions (Lee et al., 2004), or sensors (Ghosh et al., 2003) requires the knowledge of changes in electronic properties of nanotubes under external electric or magnetic fields. However, it is also important to realize that carbon nanotube properties can be tuned by such fields to reach a desirable functionality. The cylindrical structure of nanotubes suggests two high symmetry directions for application of those external fields: parallel and perpendicular to the nanotube axis (Fig. 6). Theoretical and experimental studies have shown that external electric and magnetic fields have a drastic effect on electronic and magnetic properties of carbon nanotubes (Lai, et al., 2008; Li. & Lin 2006; Minot et al., 2004). The general pattern of external electric and magnetic fields is an electronic band structure modulation with semiconductor-metal or metal-semiconductor transition, as well as lifting the degeneracy of sub-bands (Fig. 6).

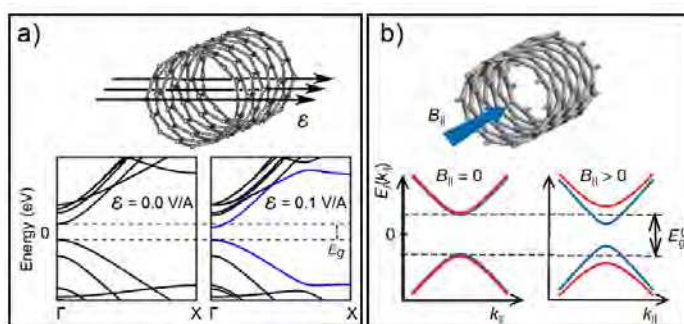


Fig. 6. a) Prospective view of (8,0) nanotube under transverse external electric field (top) and band structure changes under $\mathcal{E}=0 \text{ V/\AA}$ and $\mathcal{E}=0.1 \text{ V/\AA}$ external electric field (bottom). b) Prospective view of nanotube in the presence of magnetic field along nanotube axis (top) and band structure changes under magnetic field from (Minot et al., 2004). The magnetic and electric fields lift of the degeneracy of the band structure.

As Fig.6 shows, the energy band gap decreases, and the degeneracy of the energy bands around E_F disappears with the increase of the strength of applied fields. Application of the external electric field parallel to the nanotube axis has attracted a lot of attention because of the excellent field emission properties of carbon nanotubes (Jonge et al., 2004). Such properties have effectively been used in prototype devices such as flat panel display (Choi et al., 1999), x-ray tube (Sugie et al., 2001), and scanning x-ray source (Zhang et al., 2005). Nevertheless, the search for new devices is ongoing. Currently, researchers are exploring the

perpendicular direction of field applications as new opportunities of controlling electronic properties of nanotubes.

The application of external magnetic field leads to metal-insulator transition in nanotubes. Moreover, the carbon nanotubes can have diamagnetic or paramagnetic characteristics which depend on their chirality and the orientation of magnetic field (Lu 1995). When the magnetic field is applied along the nanotube axis (Fig.6b), oscillations in the magnetoresistance or in the band gap can be observed due to the Aharonov-Bohm effect, which is a periodic behavior of the wave-function phase factor in the cylindrical geometry (Bachtold et al., 1999; Lee et al., 2000). The Zeeman effect has been found to cause metallization of carbon nanotubes at certain values of the magnetic flux (Jiang et al., 2000). However, perpendicularly applied magnetic field has a different effect on the electronic structure of nanotubes. It opens the band gap at a weak strength and closes that band gap at a high strength of magnetic field for zigzag nanotube. When the magnetic length $l = \sqrt{ch/eH}$ is smaller than the nanotube circumference, the formation of Landau level formations at high magnetic fields closes the band gap, while those levels do not appear in small magnetic fields (Ajiki & Ando 1996). The application of external electric or magnetic fields has also been used in experimental alignment of carbon nanotube samples (Kordas et al., 2007; Kumar et al., 2003).

3. Calculations Method and Model

3.1 Method

First principal simulations are considered to be a state of the art approach for nanoscale design. Such simulations allow investigating a large variety of systems, while these can be very difficult to recreate in actual experiments. They are a powerful tool to explore the functional properties of prospective nanodevices. Among atomistic simulation methods, density functional theory (DFT) is the most successful quantum mechanical technique for calculating the electronic structures of many materials. DFT results are found in a satisfactory agreement with numerous experimental data. Our main method of investigation is based on self-consistent DFT calculations within the local density approximation (LDA) for the exchange-correlation functional implemented within the Vienna Ab Initio Simulation Package (VASP) (Kresse & Furthmuller 1996). The code uses plane-wave basis set and it is a periodic supercell approach. The core electrons of the atoms are treated by ultrasoft Vanderbilt pseudopotentials or by the projector-augmented wave method (Kresse & Joubert 1999). This DFT method is rescalable for large systems, and it requires relatively small plane-wave basis set for each atom in the calculation. It also allows the application of external electric fields in the system (Neugebauer & Scheffler 1992). Over the last decay, DFT-LDA has been a useful model in studying large graphitic structures. It provides an accurate description of the electronic structure along the graphite planes and nanotube axis, where the electronic structure is characterized by sp^2 orbitals of the carbon atoms (Kolmogorov & Crespi 2005; Shtogun et al., 2007; Woods et al., 2007). Based on its past success, we utilize DFT-LDA for our studies. The calculation criteria for relaxation of the atom positions have been 10^{-5} eV for the total energy and 0.005 eV/Å for the total force. Spin-polarization effects are also included in the study for defective carbon nanotubes.

3.2 Model

As a model for investigating the combined effect of radial deformation and defects, we study a zigzag (8,0) single wall carbon nanotube. To avoid the interaction between nearest-neighbor defects we construct a supercell consisting of four unit cells along the z -axis of the nanotube which has the length of 17.03 Å after relaxation. The radial deformation is simulated by applying stress to the cross section of the nanotube along the y -direction from both sides. Consequently, the nanotube is compressed along the y -direction and extended along the x -direction (Fig. 2a-b). The nanotubes are squeezed by two types of strain. The first one is deforming the nanotube between two hard surfaces with a cross section smaller than the nanotube one, which we call "Peanut" deformation (Fig. 2c). The second one represents squashing the nanotube between two hard surfaces with a cross section larger than the nanotube one, which we call "Flat" deformation (Fig. 2d). Such deformations are modeled by fixing the y -coordinates of the top and bottom rows at low curvature in Peanut and Flat structures, while the rest of the atoms are free to relax. We show that the (8,0) nanotubes can undergo large radial deformations - up to $\epsilon_{yy}=75\%$ and $\epsilon_{yy}=65\%$ for Peanut and Flat deformation, respectively (Shtogun & Woods 2009a).

After the radial deformation, defects, such as a Stone-Wales defect, nitrogen impurity, or mono-vacancy are introduced on the high curvature of the nanotube. Experimentally this can be achieved, for example, by deforming the tube using an atom force microscope and then intentionally introducing defects using electron or ion irradiation methods. The radially deformed carbon nanotube with or without defects has an elastic response even under high degree of squeezing. When the applied stress is removed, the nanotube comes back to its original circular cross-sectional form regardless of the defect presence.

To study the combined effect of radial deformation and an external electric field we focus on zigzag semiconducting (8,0) and metallic (9,0) single wall carbon nanotubes. The constructed supercell consists of one unit cell along z -axis with length of 4.26 Å for the (8,0) and 4.25 Å for the (9,0) nanotubes after relaxation. The external applied electric field is generated by a saw-tooth electric potential (Neugebauer & Scheffler 1992) in three different directions: \mathcal{E}_x and \mathcal{E}_y along x and y -axes, respectively, and \mathcal{E}_{45° along 45° from the x -axis (Shtogun & Woods 2009b).

4. Carbon Nanotubes under Two External Factors

Many devices associated with different applications are based on the unique properties of carbon nanotubes and the opportunity of controlling them. The search for new methods to modulate nanotube properties has led to the introduction of deformation, mechanical defects, and external fields. Reaching the desirable properties of nanotubes under one external factor, however, can be difficult in device engineering. To overcome such difficulties, researchers now consider how more than one external factors can alter the carbon nanotube properties. Thus, it is important to build fundamental understanding of the combination of more than one external stimulus by starting with applying two stimuli simultaneously.

Studies have shown that the combination of radial deformation and impurity or vacancy, for example, can facilitate tuning electronic properties of nanotubes (Fagan et al., 2003; Fagan et al., 2004). As we have shown above, the radial deformation causes the closing of band gap in semiconductor nanotubes but how fast this band gap is closed can be controlled by various

defects such as impurities and vacancies (Fagan et al., 2004). Radial deformation produces two regions with high and low curvatures (Fig.2b). As a result, the atoms on the high curvature tend to have sp^3 configuration, and they are more strained than the ones on the low curvature with sp^2 configuration. It makes it easier to create the defect on the high curvature in comparison to the low one. The flexibility in localization of the defect in radially deformed nanotubes gives more control over nanotube properties.

Band gap modulation can also be achieved by combining external electric fields and defects in nanotubes. This is of particular interest in application of nanotubes in field-effect transistors since the current can be turned off or on by applying external electric field. Such combination provides an opportunity to identify presence of defects in carbon nanotubes. Rotating nanotube in external electric field provides different responses in different directions (Tien et al., 2005). Fig. 7 shows the presence of a vacancy defect in (10,0) nanotubes with an applied external electric field for various directions. We can see that the value of the band gap can be controlled by the presence of vacancy, strength, and direction of electric field. It is interesting that usually semiconducting tubes are used in nanoelectronics. Metallic nanotubes have been discarded because their resistance is not sensitive to gate voltage or transverse electric field (Li et al., 2003). New views on metallic nanotube application are considered due to the combined effect of external electric field and impurities, which allows tuning the resistance by two orders of magnitude. The origin of this change comes from the backscattering of conduction electron by impurities, and it strongly depends on the strength and orientation of the applied electric field (Son et al., 2005).

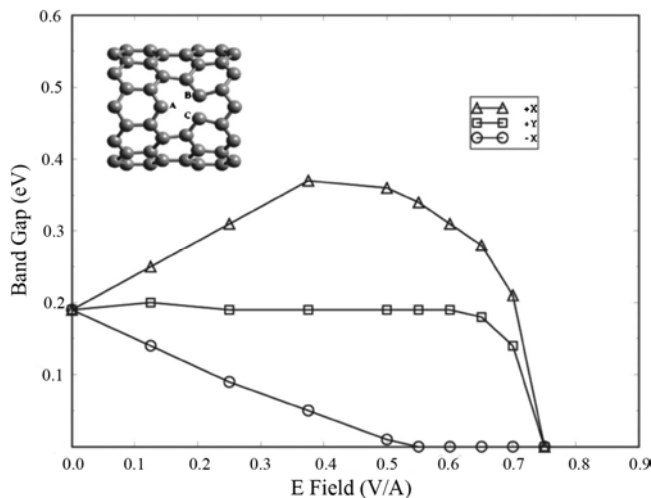


Fig. 7. Energy band gap evolution as a function of external electric field in three directions such as +x-axis, -x-axis, and +y-axis for vacancy defect in (10,0) nanotube with 79 carbon atoms from (Tien et al., 2005). The insert shows the optimized structure of vacancy defect.

Nowadays, most magnetic materials are based on d and f elements. However, as we mentioned above, sp^2 and sp^3 hybridization due to mechanical defects (vacancy and impurity) can also induce magnetism in carbon nanotubes. This is of great importance for

nanotube applications in magnetic and spintronic devices. Magnetism can be further influenced by the combined effect of mechanical deformation and defects. The strong magneto-mechanical coupling has been shown in defective nanotubes under mechanical deformation (Zheng & Zhuang 2008). It can increase or decrease the magnetic moment and cause changes in the spin transport. To further investigate this, we have explored energetic, structural, magneto-mechanical, and electronic changes in carbon nanotubes under combined effect of radial deformation and external electric field along with radial deformation and different defects.

4.1 Structural Changes in Radially Deformed and Defective Carbon Nanotubes

In this section we analyze the changes in the carbon nanotube structure under radial deformation and various defects under two types of deformation - Peanut and Flat. The main focus is on the bonds on the high curvature and the bonds comprising the defects (Fig. 4). When the perfect nanotube is radially deformed, the bonds along the nanotube axis (C-C1) decrease while the curvature bonds (C-C2) increase to reduce the strain on the high curvature (Fig. 8a). Under moderate radial deformation ($\epsilon_{yy} < 50\%$) there is no significant difference between Peanut and Flat deformation. However, at high deformation ($\epsilon_{yy} > 50\%$) the difference becomes more evident since the Flat deformation applies much more distortion on the high curvature rather than the Peanut does. As a result, the bonds on the high curvature change more in Flat than Peanut deformation, while there are no changes along nanotube axis (Fig. 8a). It is worth mentioning that in the region of ($\epsilon_{yy} \sim 20 \div 25\%$), the (8,0) nanotube shows interesting changes in the structure, which can be seen in the jump of the bond length profile. Later, there will be more discussion of this jump due to the admixture of different orbitals from the C atoms.

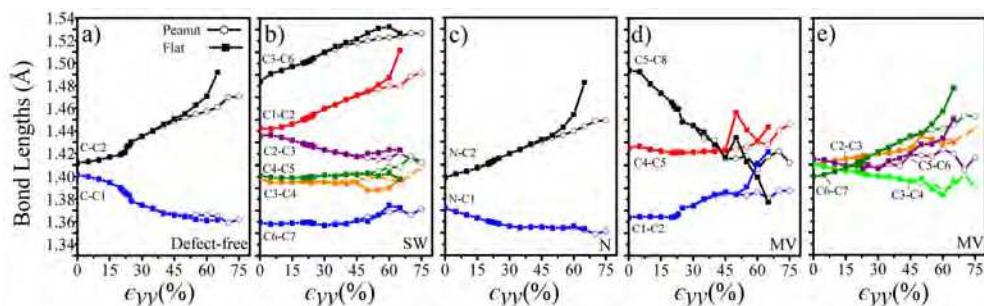


Fig. 8. (8,0) nanotube bond length evolution as a function of applied strain ϵ_{yy} with a) no defect, b) with a Stone-Wales defect, c) with a nitrogen impurity, d) and e) with a mono-vacancy.

Energetically favorable configuration of Stone-Wales defect happens when two heptagon rings align with the nanotube axis (Fig. 4b). Fig. 8b) shows the evolution of various bond changes as a function of ϵ_{yy} . Both, Peanut and Flat, deformations produce almost the same changes in the defect bond lengths with the exception of the C1-C2 bond. In fact, the bonds in the heptagon rings (C1-C2, C2-C3, and C3-C6) undergo more changes than the bonds in pentagon ones (C3-C4, C4-C5, and C6-C7). Such changes are explained by the location of the heptagon rings on the high curvature because the pentagon rings are distant from it.

Moreover, the *C1-C2* functional behavior looks similar to the one for the *C-C2* in the defect-free nanotube.

The presence of a nitrogen impurity on the high curvature of the nanotube does not create much disturbance in its structure (Fig. 4c). Since the atomic size of the nitrogen atom is larger than the carbon one, it leads to the decrease in *N-C1* and *N-C2* bond lengths by 0.01 Å and 0.03 Å as compared to the *C-C1* and *C-C2* in defect-free nanotube for all ϵ_{yy} , respectively (Fig. 8c). Another evidence of small disturbance due to the nitrogen atom can be seen from the functional behavior of the *N-C1* and *N-C2* bonds, which exhibits similar dependence on ϵ_{yy} as the corresponding *C-C* bonds in the defect-free nanotube (Fig. 8a).

Removing a carbon atom from the carbon network creates a vacancy leaving three dangling bonds behind. Such configuration is not stable, and it undergoes reconstruction with the formation pentagon and nonagon along the axis of zigzag nanotube (Fig. 4d). On the contrary to the previous cases (defect-free, Stone-Wales, and nitrogen impurity) where the bond lengths show continuous behavior, vacancy has more dramatic dependence as a function of deformation ϵ_{yy} (Fig. 8d-e). In particular, when the distance between the two low curvatures becomes comparable with graphite interplanar distance, there are some relatively “sudden” jumps and dips in bond lengths for Flat deformation. We again observe that most changes in the bond lengths happen on the high curvature. For instance, the bond lengths of *C1-C2* and *C6-C7* increase by 0.06 Å and 0.08 Å, respectively, while the *C5-C8* decreases by 0.11 Å for the Flat deformation.

As a result, the presence of mechanical defects causes the structural changes in nanotubes where nitrogen impurity creates the lowest perturbation in nanotube network while the mono-vacancy – the largest one.

4.2 Characteristic Energies of Deformation and Defect Formation in Carbon Nanotubes

The structural changes described above lead to changes in deformation and defect formation energies. We introduce the characteristic energies of radial deformation and defect formations. The energy required to perform radial deformation is defined as:

$$E_{\epsilon_{yy}}^f = E_{\epsilon_{yy}} - E \quad (3)$$

where $E_{\epsilon_{yy}}$ is the total energy for the deformed nanotube and E is the total energy for the undeformed perfect nanotube. Fig. 9 shows the deformation energy for (8,0) and (9,0) carbon nanotubes as a function of ϵ_{yy} . The deformation energy has non-linear dependence and it rises with the increasing ϵ_{yy} showing that higher deformation requires more energy to overcome strain energy on the high curvature. On the other hand, the deformation energy for (8,0) nanotube is steeper than for (9,0) due to the larger curvature effect in (8,0) nanotube as compared to the (9,0) one.

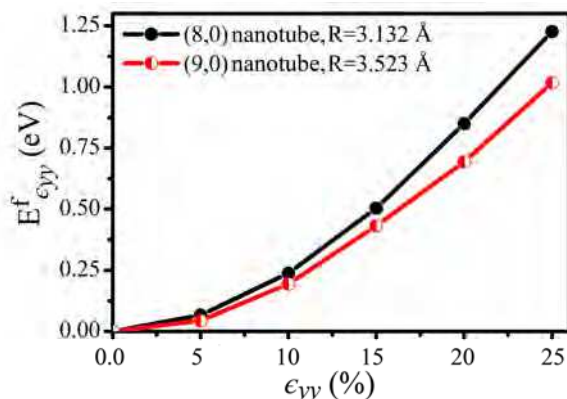


Fig. 9. The deformation energy as a function of radial deformation ϵ_{yy} for one unit cell of (8,0) and (9,0) nanotubes.

The defect formation energies for the Stone-Wales defect, nitrogen impurity, and vacancy at the high curvature of the radially deformed nanotube are calculated, respectively as:

$$E^f_{\epsilon_{yy}/SW} = E_{\epsilon_{yy}/SW} - E_{\epsilon_{yy}} \tag{4}$$

$$E^f_{\epsilon_{yy}/N} = E_{\epsilon_{yy}/N} - E_{\epsilon_{yy}} - \mu_N + \mu_C \tag{5}$$

$$E^f_{\epsilon_{yy}/MV} = E_{\epsilon_{yy}/MV} - E_{\epsilon_{yy}} + \mu \tag{6}$$

where $E_{\epsilon_{yy}/SW,N,MV}$ are the total energies for the deformed nanotube with the appropriate defect (SW - Stone-Wales, N - nitrogen impurity, and MV - mono-vacancy), $\mu_{N,C}$ are the chemical potentials for a free nitrogen and carbon atoms, respectively, and μ is the chemical potential of a carbon atom in the nanotube (energy per C atom in the supercell).

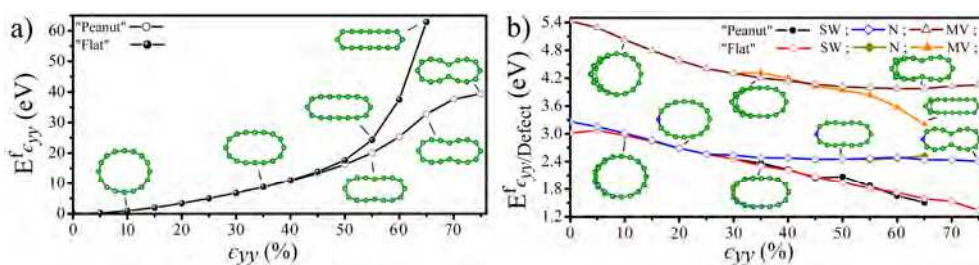


Fig. 10. The energy of a) deformation and b) defect formation as a function of ϵ_{yy} for Peanut and Flat deformations in (8,0) nanotube. Cross-sectional views of the deformed and defective (8,0) nanotubes are also provided.

Applied radial deformation of up to $\epsilon_{yy} < 35\%$ transforms the circular (8,0) nanotube to an elliptical-like one (Fig. 2b). Further increase of $\epsilon_{yy} > 35\%$ results in Peanut or Flat structures.

As it can be seen from Fig. 10a, the deformation energy becomes more distinctive between Peanut and Flat deformations for higher radial stress - $\epsilon_{yy} > 45\%$. What actually happens for high deformation is that for the Peanut deformation only one row set on the top and the bottom of low curvatures are brought together. Consequently, there are no significant changes on the high curvature and elongation along a -axis (Fig. 2c). The Flat deformation, however, has five rows of atoms from top and bottom on the low curvatures brought together (Fig. 2d). As a result, it leads to major changes on high curvature and appropriate elongation along a -axis (Fig. 2d). Meanwhile, radial deformation energy shows steeper increase in Flat than in Peanut deformation. In addition, there is a repulsion between two low curvatures of nanotube at $\epsilon_{yy} > 50\%$, where separation distance becomes smaller than graphite interplanar distance. The repulsion is stronger for Flat rather than Peanut deformation because fewer atoms are brought together in Peanut as compared to Flat deformation.

Fig. 10b also shows variations in the defect formation energy as a function of the deformation. All energies $E_{\epsilon_{yy}/SW,N,MV}^f$ decrease for all types of defects as ϵ_{yy} increases.

Therefore, the defect formation occurs much easier in radially deformed carbon nanotubes than in the undeformed ones. This has been shown for Si doping of carbon nanotubes (Fagan et al., 2004). Analysis of defect formation energies shows that the lowest amount of energy is required to produce Stone-Wales defect, more energy is needed to make nitrogen impurity and the most energy-expensive is the vacancy formation at high curvature of carbon nanotubes. There is a small difference between Peanut and Flat deformations for Stone-Wales defect and nitrogen impurity, while this difference is significant for mono-vacancy. It relates to the fact that Stone-Wales and nitrogen impurity create small disturbance in nanotube structure for both deformations where the C-C bonds in mono-vacancy exhibit more dramatic changes for the Flat than Peanut deformations (Fig. 8d-e). Thus it is easier to break the three bonds to form a mono-vacancy after squashing between two wide surfaces as compared to the case of two narrow ones (Fig. 2c-d). As a result, the higher the deformation ϵ_{yy} is, the easier it is to make defects in carbon nanotube structure.

4.3 Electronic and Magnetic Properties of Carbon Nanotubes under Combined Effect of Radial Deformation and Defects

One of the main questions we consider here is what electronic response carbon nanotubes show under the combined effect of radial deformation and different defects. We address this issue by analyzing the modulation of the band gap E_g of defect-free and defective (8,0) nanotube under radial deformations ϵ_{yy} (Fig. 11). Initially, the defect-free (8,0) nanotube is a semiconductor with $E_g = 0.55$ eV. Applying radial deformation leads to decreasing of E_g until its closure at $\epsilon_{yy} = 23\%$ where semiconductor-metal transition occurs. As we observed earlier, this semiconductor-metal transition is reflected in discontinuous change in the C-C1 and C-C2 bonds (Fig. 8a). On the other hand, it corresponds to a strong σ - π hybridization on high curvature which causes structural and semiconductor-metal transformations in (8,0) nanotube. Interestingly, such transition arises before (8,0) nanotube undergoes Peanut or Flat deformations. Further increase of radial deformation does not open second band gap in the (8,0) nanotube.

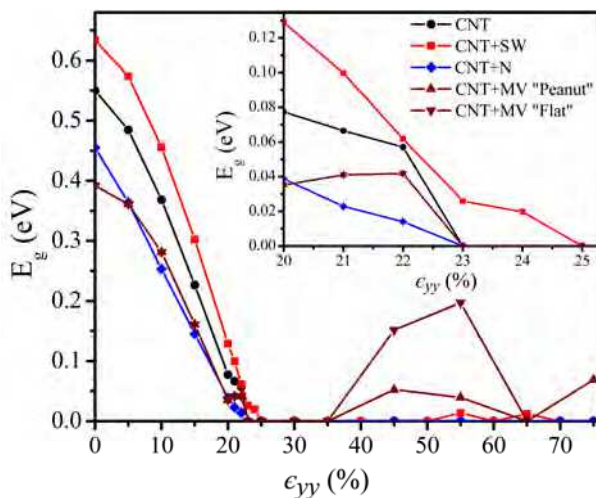


Fig. 11. Energy band gap E_g of perfect and defective (8,0) nanotubes as a function of radial deformation ϵ_{yy} . Insert shows the semiconductor-metal transition in (8,0) nanotube in detail.

The presence of defects at high curvature tunes the value of band gap in nanotubes. For instance, Stone-Wales defect increases E_g , while E_g decreases for nitrogen impurity and mono-vacancy as compared to defect-free nanotube at $\epsilon_{yy}=0\%$. Applying radial deformation to the defective nanotube has shown similar trends as in defect-free nanotubes (Fig. 11). Moreover, the semiconductor-metal transition happens at the same degree of deformation $\epsilon_{yy}=23\%$ for nitrogen impurity and mono-vacancy. However, it occurs at $\epsilon_{yy}=25\%$ for Stone-Wales defect. Further increasing deformation opens the band gap in nanotube with mono-vacancy and Stone-Wales defect again, while nanotube with nitrogen impurity remains metallic for all deformations. In addition, the band gap can be modulated by Peanut or Flat deformations at high deformation. Still, we can see that strong σ - π hybridization is a major factor in semiconductor-metal transition in defective nanotubes but defect-deformation coupling is significant for further opening of the band gap at high deformations.

To elucidate the mechanism of semiconductor-metal transformation in defect-free and defective nanotubes we carry out comprehensive analysis of the electronic structure changes for various cases. The applied radial deformation removes the degeneracy in sub-bands of defect-free nanotubes (Fig. 12a). Increasing ϵ_{yy} causes the lowest conduction band and the highest valence band to move towards the Fermi level. They cross the Fermi level at the point different than Γ for $\epsilon_{yy}=23\%$. The further deformation leads to the shift of crossing point with E_F towards the X point. For sufficiently large $\epsilon_{yy}>50\%$, multiple crossings at the Fermi level from higher conduction and lower valence bands occur, which improve metallization of nanotubes and increase the density of states at the Fermi level. Initial analysis reveals that all atoms of carbon network equally contribute to the energy band. However, this input changes with applied deformation. The atoms from high curvature have the main contribution to the energy bands around the Fermi level. For $\epsilon_{yy}>50\%$ the atoms from the low curvature in the Peanut deformation (top and bottom rows) also contribute to the energy bands at the Fermi level.

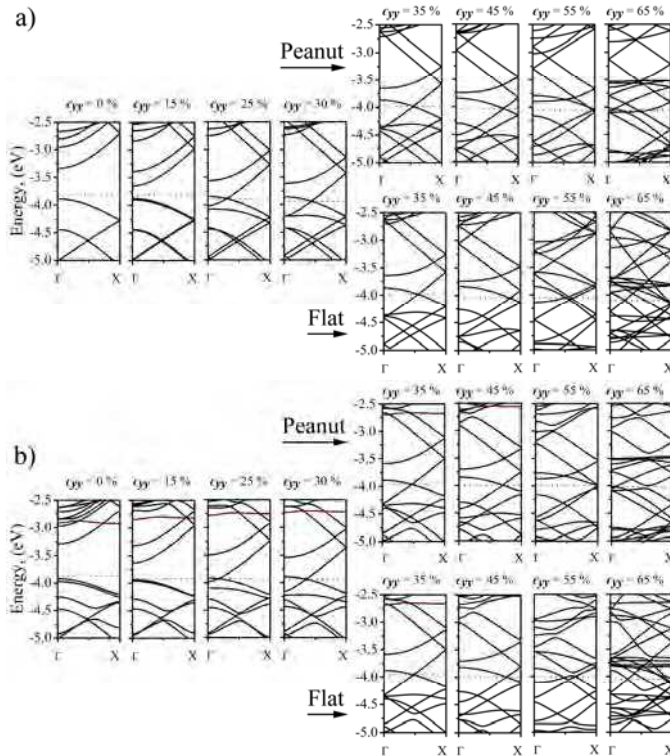


Fig. 12. The energy band structure of a) defect-free (8,0) nanotube, b) (8,0) nanotubes with Stone-Wales defect at high curvature site for several degrees of ϵ_{yy} . The red level is associated with the Stone-Wales defect.

The band structure evolution of the deformed (8,0) nanotube with a Stone-Wales defect shows similar behavior as compared to the defect-free one (Fig. 12b). However, Stone-Wales defect increases initial value of band gap and introduces flat defect level in the conduction band at $E \approx -2.9$ eV (in red). Under applied radial deformations $\epsilon_{yy} > 0\%$, this flat level starts to move away from the Fermi level while increasing σ - π hybridizations brings the lowest conduction and the highest valence bands closer together. Small band gap $E_g \approx 0.01$ eV opens up for the Peanut deformation at $\epsilon_{yy} = 55\%$ and $\epsilon_{yy} = 65\%$. There is no such opening for Flat deformation, and the band gap remains closed. The analysis of conduction and valence bands reveals that the lowest conduction bands consist of the orbital from defect atoms where σ - π hybridizations is significant.

The applied radial deformation induces nonuniform charge distribution on the nanotube surface (Fig. 13). For a defect-free nanotube, the charge accumulation appears on the high curvature. Even more irregular allocation is caused by Peanut and Flat deformations (Fig. 13a-c). Stone-Wales defect creates local disturbance in the nanotube structure, which reduces charge accumulation on the defect itself, except for the C6-C7 bond even though it is on the high curvature. Most of the charge is gathered around the atoms surrounding Stone-Wales defect (Fig. 13d-f).

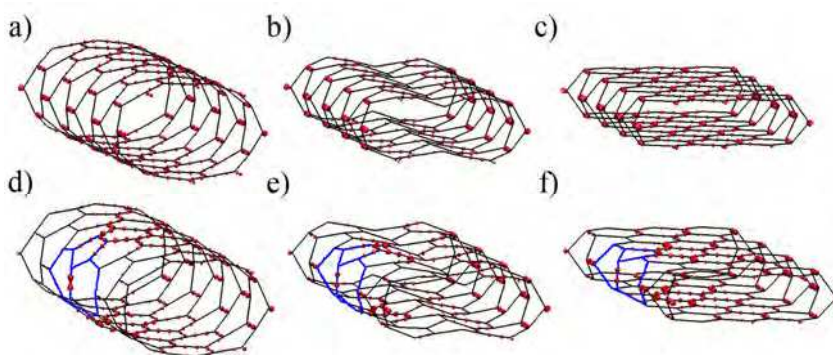


Fig. 13. Total charge density plots with isosurface value is $0.0185 e/\text{\AA}^3$ for a) defect-free (8,0) nanotube with $\epsilon_{yy}=25\%$, b) Peanut structure with $\epsilon_{yy}=65\%$, c) Flat structure with $\epsilon_{yy}=65\%$, and d) (8,0) nanotube with Stone-Wales defect with $\epsilon_{yy}=25\%$, e) Peanut structure with $\epsilon_{yy}=65\%$, f) Flat structure with $\epsilon_{yy}=65\%$.

The effects of nitrogen impurity and mono-vacancy in radially deformed nanotubes have been investigated in terms of Density of States (DOS) for different ϵ_{yy} . Since the nitrogen atom supplies one extra electron in nanotube, and mono-vacancy provides dangling bond, the calculations include spin-polarized effect to account for magnetic effect in nanotubes. The possibility of magnetism in nanotube has been predicted by other authors (Lim et al., 2007; Orellana & Fuentealba 2006; Wu & Hagelberg 2009). The density of states of nitrogen doped nanotubes is responsive to the concentration of impurities (Orellana & Fuentealba 2006). Increasing the impurity concentration more than 1% provides a flat level in the band gap. In our calculation we do not observe any flat level because the nitrogen concentration is 0.78% (Fig. 14a). As the radial deformation ϵ_{yy} increases, the band gap decreases, and the conduction and valence bands move towards the Fermi level. For $\epsilon_{yy}>45\%$, the DOS for Peanut and Flat deformation raises around the Fermi level which suggests that the nanotube shows more metal-like behavior.

The nitrogen impurity contributes significantly to conduction band in the vicinity of the Fermi level which is partially occupied. The highest valence band consists of contribution from atoms on the high curvature. The extra nitrogen e^- induces spin-polarization effects (magnetism) in the nanotube electronic structure at $\epsilon_{yy}=0\%$ and sharp features in the DOS for spin "up" around ~ -2.8 eV (Fig. 14a). As ϵ_{yy} increases, the spin-polarized effect is overtaken by σ - π hybridization. Eventually, it completely disappears at $\epsilon_{yy}>25\%$ except for at $\epsilon_{yy}=65\%$ for Flat deformation. Thus, applied radial deformation provides the opportunity to control not only electronic but also magnetic properties of nanotubes. To elucidate this effect further, we investigate changes in local magnetic moment m under ϵ_{yy} (Fig. 14b). For small deformations m increases with a maximum at $\epsilon_{yy}=5\%$ and then it reduces to $m=0$ at $\epsilon_{yy}=25\%$ when the nanotube becomes almost a metal ($\epsilon_{yy}=23\%$). However, complicated magneto-mechanical coupling produces large magnetic moment $m=0.92 \mu_B$ (not shown on Fig. 14b) at $\epsilon_{yy}=65\%$. It gives evidence of new methods of tuning nanotube properties and complex interrelation between defects and deformations.

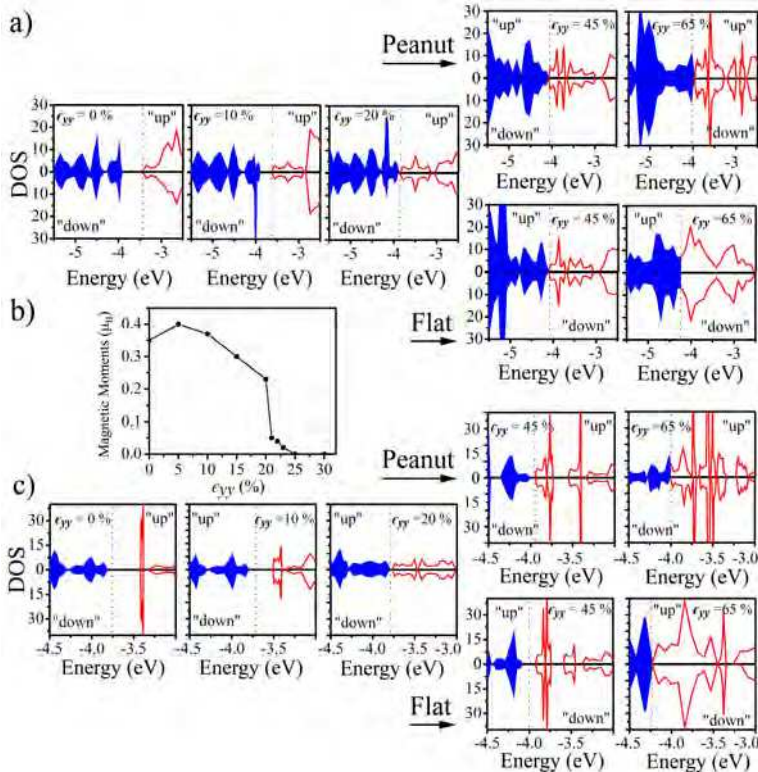


Fig. 14. a) Total Density of States for spin "up" and "down" carriers of (8,0) nanotube with a substitutional nitrogen impurity on its high curvature at different ϵ_{yy} for Peanut and Flat structures. b) The magnetic moment of the (8,0) nanotube with the nitrogen impurity as a function of ϵ_{yy} . c) Total Density of States for spin "up" and "down" carriers of (8,0) nanotube with mono-vacancy defect on its high curvature at different ϵ_{yy} for Peanut and Flat structures.

Finally, we consider a radially deformed (8,0) nanotube with a mono-vacancy (Fig. 14c). The presence of mono-vacancy is manifested in a sharp localized peak around -3.41 eV in the DOS conduction region for the spin "up" and "down" at $\epsilon_{yy}=0\%$. This state mainly consists of contributions from the mono-vacancy atoms. As the deformation progresses, the peak intensity decreases and becomes broader, and peak location moves closer to the Fermi level due to σ - π hybridization from the nanotube atoms on high curvature along with the C atoms of mono-vacancy. Such process repeats again for $\epsilon_{yy}>40\%$, where sharp peaks around the Fermi level occur and become wider and sharper with increasing ϵ_{yy} . The major contribution to these peaks comes from dangling bond atom - C1 and the C atoms of the pentagon ring of mono-vacancy (Fig. 4d). DOS for spin "up" and "down" demonstrates that there is no spin-polarized effect in radially deformed nanotubes with mono-vacancy for all ϵ_{yy} except $\epsilon_{yy}=65\%$ in Peanut deformation where a small magnetic moment $m=0.04 \mu_B$ has been found. These results are in partial agreement with previously reported findings that zigzag nanotubes with mono-vacancy do not show magnetic response for given orientation of

defect (Berber & Oshiyama 2006). However, the appearance of magnetism at $\epsilon_{yy}=65\%$ can originate from several reasons such as uncoordinated C atom with a localized unpaired spin, concentration of vacancies, nanotube chirality, sp^3 pyramidization, and related bond length changes, as well as vacancy location with respect to the nanotube structure (Ma et al., 2004; Orellana & Fuentealba 2006; Zheng & Zhuang 2008). Another explanation of the magnetism in radially deformed nanotubes with mono-vacancy is the magnetic flat-band theory together with σ - π hybridization (Fujita et al., 1996; Nakada et al., 1996). The presence of flat bands around the Fermi level leads to increased electron-electron interaction and results in the occurrence of magnetic polarization which is common for edge states in zigzag nanoribbons (Fujita et al., 1996; Nakada et al., 1996). We can consider a mono-vacancy on the high curvature and large deformations such edge states. Our results suggest that there is a complex relation among mechanical, electric, and magnetic coupling in radially deformed nanotubes with the mono-vacancy.

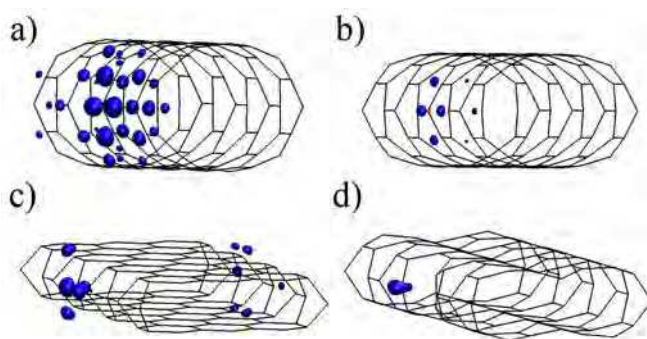


Fig. 15. Spin density isosurface plots for a) (8,0) nanotube with nitrogen impurity for $\epsilon_{yy}=10\%$ at $0.004 \mu_B/\text{\AA}^3$, b) (8,0) nanotube with nitrogen impurity for $\epsilon_{yy}=20\%$ at $0.004 \mu_B/\text{\AA}^3$, c) Flat (8,0) nanotube with nitrogen impurity for $\epsilon_{yy}=65\%$ at $0.0122 \mu_B/\text{\AA}^3$, d) Peanut (8,0) nanotube with mono-vacancy for $\epsilon_{yy}=65\%$ at $0.018 \mu_B/\text{\AA}^3$.

Further insight in the nanotube magnetism can be gained by exploring the spin density distribution for various deformations ϵ_{yy} (Fig. 15). Initially extra nitrogen e^- is localized on the defect site but increasing deformation obliterates this localization. As an example, the unpaired e^- is much more delocalized at $\epsilon_{yy}=20\%$ in comparison to the $\epsilon_{yy}=10\%$ case, where the e^- spin density localized around the impurity site is much more intense. Similar behavior has been reported for semiconducting nanotubes, where the nitrogen e^- is localized around the impurity, while for metallic nanotube it is completely delocalized (Nevidomskyy et al., 2003). However, the e^- spin localization around the impurity appears again at $\epsilon_{yy}=65\%$ in Flat deformation, where the nanotube is a metal, but the magnetic moment has the highest value of $-m=0.92 \mu_B$. Moreover, similar localization of the spin density happens around the dangling bond in the nanotube with mono-vacancy $\epsilon_{yy}=65\%$. This suggests that the uncoordinated C atom with unpaired spin is vital in the magnetic properties of defective and deformed nanotubes.

4.4 Electronic Properties of Carbon Nanotubes under Radial Deformation and an External Electric Field

Next, we explore the electronic properties of radially deformed nanotubes in an external radial electric field. We focus on the modulation of the band gap by an external electric field in nanotubes with various degrees of deformation. As we have already seen from earlier discussion, applying radial deformation causes the metal semiconductor transition in semiconductor nanotubes and causes opening and closing of a band gap in metallic nanotubes because of the $\sigma - \pi$ hybridization from the high curvature regions. Fig. 16a-b show these dependences in semiconductor (8,0) and semi-metal (9,0) carbon nanotubes as a function of ϵ_{yy} . The same behavior can be achieved by the application of an external electric field to undeformed (8,0) and (9,0) nanotubes. E_g dependences in Fig. 16c-d and Fig. 16a-b look similar. However, the semiconductor-metal transition happens faster for the (8,0) nanotube over a shorter field strength interval as compared to the (9,0) nanotube. In this case, E_g for (8,0) nanotube is closed at $\mathcal{E}=0.4 \text{ V/\AA}$, while for (9,0) tube the closure occurs at $\mathcal{E}=0.8 \text{ V/\AA}$. Therefore, we can obtain the same electronic characteristics of nanotubes from radial deformation and the applied external electric field. In addition, it provides the flexibility of controlling nanotube properties at different circumstances.

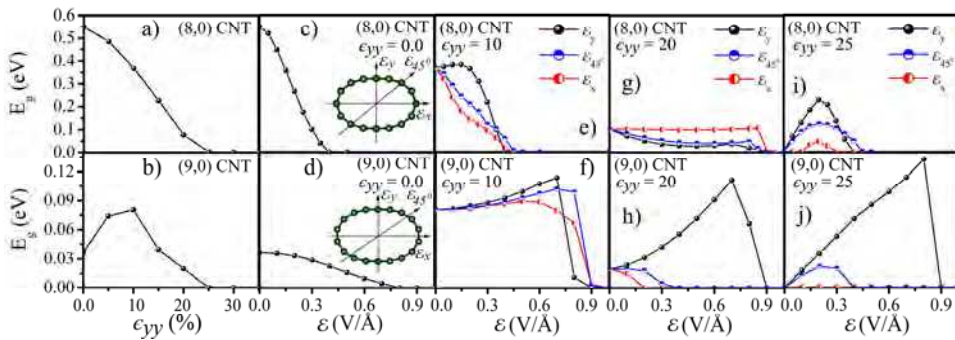


Fig. 16. E_g as a function of ϵ_{yy} for a) (8,0) and b) (9,0) nanotubes; E_g as a function of \mathcal{E} for c) (8,0) at $\epsilon_{yy}=0\%$; d) (9,0) at $\epsilon_{yy}=0\%$; e) (8,0) at $\epsilon_{yy}=10\%$; f) (9,0) at $\epsilon_{yy}=10\%$; g) (8,0) at $\epsilon_{yy}=20\%$; h) (9,0) at $\epsilon_{yy}=20\%$; i) (8,0) at $\epsilon_{yy}=25\%$; j) (9,0) at $\epsilon_{yy}=25\%$. The insert indicates electric field directions as follows: \mathcal{E}_x is along x -axis, \mathcal{E}_y -along y -axis, and \mathcal{E}_{45° -along 45° from x -axis in x - y plane.

The symmetry of the nanotube is decreased under applied radial deformation. Consequently, the x and y directions of the cross section are not equivalent any more (Fig. 2b). It has been shown before that electronic structure of the defective nanotube depends on the orientation of external electric field (Tien et al., 2005). Here, we analyze the E_g evolution of the deformed (8,0) and (9,0) nanotubes under \mathcal{E} along x , y -axes and the 45° direction in the x - y plane (insert in Fig. 16c-d).

Radially deformed (8,0) nanotube at $\epsilon_{yy}=10\%$ still has a relatively large band gap - $E_g = 0.37 \text{ eV}$, which decreases under applied electric field and vanishes at $\mathcal{E} \sim 0.45 \text{ V/\AA}$ for all three directions. Each E_g dependence has distinct profile for $\mathcal{E} < 0.4 \text{ V/\AA}$. E_g initially increases and

then starts to decrease for y -direction. However, it sharply decreases for x -direction, and it shows intermediate, almost linear, decline for 45° -direction (Fig.16e). At $\epsilon_{yy}=20\%$ the applied electric field has a small effect on E_g over relatively long range of electric field strength for all directions until it closes E_g at $\mathcal{E}\sim 0.8$ V/Å (Fig. 16g). The (8,0) nanotube becomes metallic at $\epsilon_{yy}=25\%$ but applied electric field opens E_g with its maximum at $\mathcal{E}\sim 0.2$ V/Å for all directions. The largest E_g is for the electric field along y -direction and the lowest - for x -direction (Fig. 16i).

On the other hand, the radially deformed (9,0) nanotube at $\epsilon_{yy}=10\%$ has the largest $E_g=0.08$ eV, which continues to increase under applied electric field in all directions until $\mathcal{E}\sim 0.6\div 0.7$ V/Å, where E_g is sharply closed (Fig. 16f). This behavior is similar for E_g in the (8,0) nanotube at $\epsilon_{yy}=20\%$. More drastic behavior of the band gap is observed at $\epsilon_{yy}=20\%$ for electric field along y -direction. The original value of the band gap increases by ~ 4 times at $\mathcal{E}=0.7$ V/Å which is followed by its rapid closure at $\mathcal{E}=0.9$ V/Å. At the same time, the weak electric field \mathcal{E} along x - and 45° - directions closes the band gap. The same dependence has been found at $\epsilon_{yy}=25\%$. The band gap reaches maximum for $\mathcal{E}=0.8$ V/Å while there is no effect of applied electric field on the band gap along x -direction.

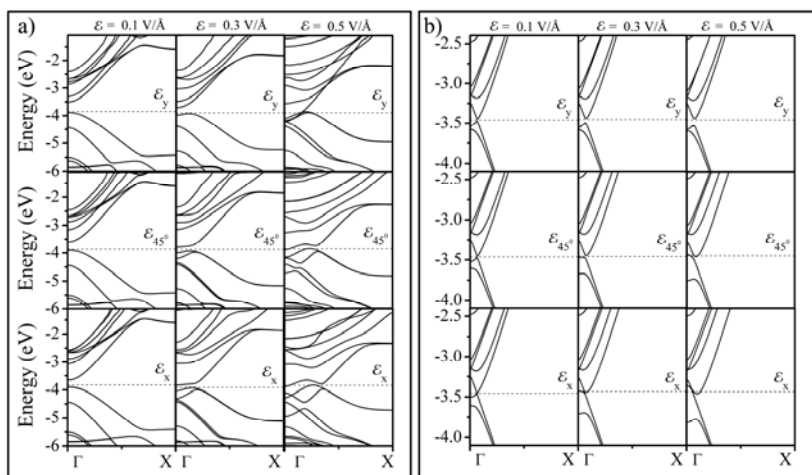


Fig. 17. Energy band structure evolutions for a) (8,0) nanotube at $\epsilon_{yy}=10\%$ and b) (9,0) nanotubes at $\epsilon_{yy}=25\%$ and electric field strength $\mathcal{E}=0.1, 0.3, 0.5$ V/Å along x, y -axis, and 45° from x -axis in x - y plane, respectively. The Fermi level is shown as a dashed line.

Better understanding of band gap modulations comes from the analysis of the electronic band structure for (8,0) and (9,0) nanotubes at $\epsilon_{yy}=10\%$ and $\epsilon_{yy}=25\%$ respectively, for several orientations (Fig. 17). The electronic level of conduction and valance bands are associated with the quantum angular momentum J which defines the rule for admixture of allowed states (Vukovic et al., 2002). It has been shown that electronic states can mix according to the selection rule $\Delta J=0, \pm 2$ for radial deformation of nanotubes (Park et al., 1999). This admixture and increasing σ - π hybridization on high curvature bring the lowest conduction and the highest valance bands - closer to the Fermi level. However, the applied electric field mixes

the electronic states in accordance with $\Delta J = \pm 1$ and also decreases the values of the band gap to its closure at E_F (Kim & Chang 2001; Li et al., 2006). The combination of radial deformation and external electric field causes the band structure modulation according to $\Delta J = 0, \pm 1, \pm 2$ selection rule and $\sigma-\pi$ hybridization on the high curvature of nanotubes. As we have seen from the band gap behavior, the strength and orientation of applied electric field with respect to the nanotube cross section are crucial for electronic properties of nanotubes. This has been reflected in the band structures for (8,0) and (9,0) nanotubes (Fig. 17). Most changes happen with the lowest unoccupied single degenerate conduction state for both (8,0) and (9,0) nanotubes. Therefore, application of electric field along x -direction (through the high curvature) has revealed the largest $\sigma-\pi$ hybridization on the high curvature. Thus, depending on the interplay between the radial deformation and electric field strength/orientation, the electronic properties of nanotubes can reveal semiconductor-metal or metal semiconductor transformation (Fig. 17).

5. Conclusion

In this chapter we discuss electronic and magnetic carbon nanotube properties under two external factors: radial deformation and various defects along with radial deformation and external electric fields. Our analysis is based on density functional theory calculations. We show that defects, such as Stone-Wales, nitrogen impurity, and mono-vacancy, create a local distortion in the carbon network. This disturbance is lowest for nitrogen, larger for Stone-Wales defect, and largest for mono-vacancy. The analysis of the characteristic energies reveals that it takes more energy to deform a smaller diameter nanotube in comparison to larger one. The larger degree of radial deformation makes it easier to introduce a defect on the high curvature of the nanotube. The Stone-Wales defect requires the lowest formation energy, while it is higher for nitrogen impurity, and it is the largest for mono-vacancy. We find that applied radial deformation causes semiconductor-metal transition in defective nanotubes at approximately the same value of applied strain ($\epsilon_{xy} = 23 \pm 25\%$) regardless of the type of defect.

The electronic structure calculations show that the main factors responsible for semiconductor-metal transition in defective nanotubes are the $\sigma-\pi$ hybridization from the high curvature and the presence of defect states around the Fermi level region. We observe that interplay between radial deformation and type of defects such as Stone-Wales defect and mono-vacancy can open the band gap again, after it has been closed due to the same factors. However, there is not such opening for the nitrogen impurity and defect-free nanotubes regardless of the type of deformation. On the other hand, mutual effect of radial deformation and defects leads to magneto-mechanical coupling in the nanotube structure because of the presence of extra an electron from the nitrogen atom and dangling bond from the mono-vacancy. The magnetic properties of nanotubes can be controlled by the degree of radial deformation. The origin of magnetic properties of nanotubes is also discussed.

The combined effect of radial deformation and external electric field is given in terms of band gap modulations, electronic band structure changes, strength of applied electric field, electric field orientation, and selection rules. We show various responses in semiconductor and metallic carbon nanotubes. The electronic structure is sensitive to the strength and electric field orientation with respect to the cross section of nanotubes. The interplay between selection rules of mixing different states in the radial deformation and applied

electric field along with σ - π hybridization controls and tunes the band gap of nanotubes. Finally, we discuss semiconductor-metal transition in semiconducting nanotubes and opening of the band gap in metallic nanotubes.

This chapter provides a comprehensive study of electronic and magnetic properties of nanotubes under two external factors. It discusses additional opportunities in controlling and tuning carbon nanotube properties for their expanded applications in current and new nano-devices.

Acknowledgments

We acknowledge the donors of the American Chemical Society Petroleum Research Fund for support of this research. In addition, the part of this work was supported by the US Army Medical Research and Materiel Command under Award No. W81XWH-07-1-0708. We also would like to acknowledge the use of the services provided by the Research Computing Core at the University of South Florida and the TeraGrid Advanced Support Program at the University of Illinois.

6. References

- Ajiki, H. & Ando, T. (1996). Energy bands of carbon nanotubes in magnetic fields. *J. Phys. Soc. Jap.*, Vol. 65, No. 2, 505-514, ISSN 00314-9015
- Ashraf, B.; Hubert, P. & Vengallatore, S. (2006). Carbon nanotube-reinforced composites as structural materials for microactuators in microelectromechanical systems. *Nanotechnology*, Vol. 17, No. 19, 4895-4903, ISSN 0957-4484
- Bachtold, A.; Strunk, C.; Salvetat, J.-P.; Bonard, J.-M.; Forro, L.; Nussbaumer, T. & Schonenberg, C. (1999). Aharonov-Bohm oscillations in carbon nanotubes. *Nature*, Vol. 397, No. 6721, 673-675, ISSN 0028-0836
- Barboza, A.; Gomes, A.; Archanjo, B.; Araujo, P.; Jorio, A.; Ferlauto, A.; Mazzoni, M.; Chacham, H. & Neves, B. (2008). Deformation induced semiconductor-metal transition in single wall carbon nanotubes probed by electric force microscopy. *Phys. Rev. Lett.*, Vol. 100, No. 25, 256804-1-4, ISSN 1079-7114
- Berber, S. & Oshiyama, A. (2006). Reconstruction of mono-vacancies in carbon nanotubes: atomic relaxation vs. spin polarization. *Physica B*, Vol. 376-377, No. 1, 272-275, ISSN 0921-4526
- Bettinger, H. (2005). The reactivity of defects at the sidewalls of single-walled carbon nanotubes: the Stone-Wales defect. *J. Phys. Chem.*, Vol. 109, No. 15, 6922-6924, ISSN 1089-5647
- Choi, W.; Chung, D.; Kang, J.; Kim, H.; Jin, Y.; Han, I.; Lee, Y.; Jung, J.; Lee, N.; Park, G. & Kim, J. (1999). Fully sealed, high-brightness carbon-nanotube field-emission display. *Appl. Phys. Lett.*, Vol. 75, No. 20, 3129-3131, ISSN 0003-6951
- Chopra, N.; Benedict, L.; Crespi, V.; Cohen, M.; Louie, S. & Zettl, A. (1995). Fully collapsed carbon nanotubes. *Nature*, Vol. 377, No. 6544, 135-138, ISSN 0028-0836
- Cohen-Karni, T.; Segev, L.; Srur-Lavi, O.; Cohen, S. & Joselevich, E. (2006). Torsional electromechanical quantum oscillation in carbon nanotubes. *Nature Nanotechnology*, Vol. 1, No. 1, 36-41, ISSN 1748-3387

- Crespi, H.; Cohen, L. & Rubio, A. (1997). In situ band gap engineering of carbon nanotubes. *Phys. Rev. Lett.*, Vol. 79, No. 11, 2093-2096, ISSN 1079-7114. Figure 5a is used with permission from American Institute of Physics, Copyright 1997.
- Czerw, R.; Terrones, M.; Charlier, J.-C.; Blase, X.; Foley, B.; Kamalakaran, R.; Grobert, N.; Terrones, H.; Tekleab, D.; Ajayan, P.; Blau, W.; Ruhle, M. & Carroll, D. (2001). Identification of electron donor stets in N-doped carbon nanotubes. *Nano Lett.*, Vol. 1, No. 9, 457-460, ISSN 1530-6984
- Droppa, R.; Hammer, P.; Carvalho, A.; Santos, M. & Alvarez, F. (2002). Incorporation of nitrogen in carbon nanotubes. *J. Non-Cryst. Solid.*, Vol. 299-302, No. 2, 874-879, ISSN 0022-3093
- Fagan, S.; da Silva, L. & Mota, R. (2003). Ab initio study of radial deformation plus vacancy on carbon nanotubes: energetics and electronic properties. *Nano Lett.*, Vol. 3, No. 3, 289-291, ISSN 1530-6984
- Fagan, S.; Mota, R.; da Silva, A. & Fazzio, A. (2004). Substitutional Si doping in deformed carbon nanotubes. *Nano Lett.*, Vol. 4, No. 5, 975-977, ISSN 1530-6984
- Fan, Y.; Goldsmith, B. & Collins, P. (2005). Identifying and counting point defects in carbon nanotubes. *Nature Materials*, Vol. 4, No. 12, 906-911, ISSN 1476-1122
- Favlo, M.; Clary, G.; Taylor II, R.; Chi, V.; Brooks, F.; Washburn, S. & Superfine, R. (1997). Binding and buckling of carbon nanotubes under large strain. *Nature*, Vol. 389, No. 6651, 582-584, ISSN 0028-0836
- Fennimore, A.; Yuzvinsky, T.; Han, W.-Q.; Fuhrer, M.; Cumings, J. & Zetti, A. (2003). Rotational actuators based on carbon nanotubes. *Nature*, Vol. 424, No. 6947, 408-410, ISSN 0028-0836
- Fujita, M.; Wakabayashi, K.; Nakada, K. & Kusakabe, K. (1996). Peculiar localized states at zig-zag graphite edge. *J. Phys. Soc. Jap.*, Vol. 65, No. 7, 1920-1923, ISSN 0031-9015
- Hashimoto, A.; Suenaga, K.; Gloter, A.; Urita, K. & Iijima, S. (2004). Direct evidence for atomic defects in graphene layers. *Nature*, Vol. 430, No. 7002, 870-873, ISSN 0028-0836
- Hertel, T.; Walkup, R. & Avouris, P. (1998). Deformation of carbon nanotubes by surface van der Waals forces. *Phys. Rev. B*, Vol. 58, No. 20, 13870-73, ISSN 1098-0121
- Gai, P.; Odile, S.; Mcguire, S.; Rao, A.; Dresselhaus, M.; Dresselhaus, G. & Colliex, C. (2004). Structural systematic in boron-doped single wall carbon nanotubes. *J. Mater. Chem.*, Vol. 14, No. 4, 669-675, ISSN 0959-9428
- Gao, G.; Cagin, T. & Goddard, W. (1998). Energetics, structure, mechanical and vibrational properties of single-walled carbon nanotubes. *Nanotechnology*, Vol. 9, No. 3, 184-191, ISSN 0957-4484
- Ghosh, A.; Sood, A. & Kumar, N. (2003). Carbon nanotube flow sensors. *Science*, Vol. 299, No. 5609, 1042-1044, ISSN 003-8075
- Giusca, C.; Tison, Y. & Silva, S. (2007). Atomic and electronic structure in collapsed carbon nanotubes evidenced by scanning tunneling microscopy. *Phys. Rev. B*, Vol. 76, No. 3, 035429-1-6, ISSN 1098-0121
- Golberg, D.; Bando, Y.; Han, W.; Kurashima, K. & Sato, T. (1999). Single-walled B-doped carbon and BN nanotubes synthesized from single walled carbon nanotubes through a substitutional reaction. *Chem. Phys. Lett.*, Vol. 308, No. 3-4, 337-342, ISSN 0009-2614

- Gulseren, O.; Yildirim, T.; Ciraci, S. & Kilic, C. (2002). Reversible band-gap engineering in carbon nanotubes by radial deformation. *Phys. Rev. B*, Vol. 65, No. 15, 155410-1-7, ISSN 1098-0121
- Itkis, M.; Yu, A. & Haddon, R. (2008). Single-walled carbon nanotube thin film emitter-detector integrated optoelectronic device. *Nano Lett.*, Vol. 8, No. 8, 2224-2228, ISSN 1530-6984
- Jiang, J.; Dong, J. & Xing, D. (2000). Zeeman effect on the electronic spectral properties of carbon nanotubes in an axial magnetic field. *Phys. Rev. B*, Vol. 62, No. 19, 13209-13215, ISSN 1098-0121
- Jonge, N.; Allieux, M.; Doytcheva, M.; Kaiser, M.; Teo, K.; Lacerda, R. & Milne, W. (2004). Characterization of the field emission properties of individual carbon nanotubes. *Appl. Phys. Lett.*, Vol. 85, No. 9, 1607-1609, ISSN 0003-6951
- Kim, Y.-H. & Chang K. (2001). Subband mixing rules in circumferentially perturbed carbon nanotubes: effects of transverse electric fields. *Phys. Rev. B*, Vol. 64, No. 15, 153404-1-4, ISSN 1098-0121
- Kolmogorov, A. & Crespi, V. (2005). Registry-dependent interlayer potential for graphitic systems. *Phys. Rev. B*, Vol. 71, No. 23, 235415-1-6, ISSN 1098-0121
- Kordas, K.; Mustonen, T.; Toth, G.; Vahakangas, J.; Uusimaki, A.; Jantunen, H.; Gupta, A.; Rao, K.; Vajtai, R. & Ajayan, P. (2007). Magnetic-field induced efficient alignment of carbon nanotubes in aqueous solutions. *Chem. Mater.*, Vol. 19, No. 4, 787-791, ISSN 0897-4756
- Krasheninnikov, A.; Nordlund, K.; Sirvio, M.; Salonen, E. & Keinonen, J. (2001). Formation of ion-irradiation-induced atomic-scale defects on walls of carbon nanotubes. *Phys. Rev. B*, Vol. 63, No. 24, 245405-1-6, ISSN 1098-0121
- Krasheninnikov, A.; Banhart, F.; Li, J.; Foster, A. & Nieminen, R. (2005). Stability of carbon nanotubes under electron irradiation: role of tube diameter and chirality. *Phys. Rev. B*, Vol. 72, No. 12, 125428-1-6, ISSN 1098-0121
- Kresse, G. & Furthmuller, J. (1996). Efficient interactive schemes for ab initio total-energy calculations using a plane-wave basis set. *Phys. Rev. B*, Vol. 54, No. 16, 11169-11186, ISSN 1098-0121
- Kresse, G. & Joubert, D. (1999). From ultrasoft pseudopotentials to the projector augmented-wave method. *Phys. Rev. B*, Vol. 59, No. 3, 1758-1775, ISSN 1098-0121
- Kumar, M.; Lee, S.; Kim, T.; Kim, T.; Song, S.; Yang, J.; Nahm, K. & Suh, E.-K. (2003). DC electric field assisted alignment of carbon nanotubes on metal electrodes. *Solid State Electron.*, Vol. 47, No. 11, 2075-2080, ISSN 0038-1101
- Lai, P.; Chen, S. & Lin, M. (2008). Electronic properties of single-walled carbon nanotubes under electric and magnetic fields. *Physica E*, Vol. 40, No. 6, 2056-2058, ISSN 1386-9477
- Lee, J.; Gipp, P. & Heller, C. (2004). Carbon nanotube *p-n* junction diodes. *Appl. Phys. Lett.*, Vol. 85, No. 1, 145-147, ISSN 0003-6951
- Lee, J.-O.; Kim, J.-R.; Kim, J.-J.; Kim, J.; Kim, N.; Park, J. & Yoo, K.-H. (2000). Observation of magnetic-field-modulated energy gap in carbon nanotubes. *Solid State Comm.*, Vol. 115, No. 9, 467-471, ISSN 0038-1098
- Lee, R.; Kim, H.; Fischer, J.; Thess, A. & Smalley, R. (1997). Conductivity enhancement in single-walled carbon nanotube bundles doped with K and Br. *Nature*, Vol. 388, No. 6639, 255-257, ISSN 0028-0836

- Leonard, F.; Jones, F.; Talin, A. & Dentinger P. (2005). Robustness of nanotube electronic transport to conformational deformations. *Appl. Phys. Lett.*, Vol. 86, No. 9, 093112-1-3, ISSN 0003-6951
- Li, T. & Lin, M. (2006). Electronic properties of carbon nanotubes under external fields. *Phys. Rev. B*, Vol. 73, No. 7, 075432-1-7, ISSN 1098-0121
- Li, Y.; Rotkin, S. & Ravaoli, U. (2003). Electronic response and band structure modulation of carbon nanotubes in a transverse electrical field. *Nano Lett.*, Vol. 3, No. 2, 183-187, ISSN 1530-6984
- Lim, S.; Li, R.; Ji, W. & Lin, J. (2007). Effect of nitrogenation on single-walled carbon nanotubes within density functional theory. *Phys. Rev. B*, Vol. 76, No. 19, 195406-1-16, ISSN 1098-0121
- Lu, A. & Pan, B. (2004). Nature of single vacancy in achiral carbon nanotubes. *Phys. Rev. Lett.*, Vol. 92, No. 10, 105504-1-4, ISSN 1079-7114. Figure 5c is used with permission from American Institute of Physics, Copyright 2004.
- Lu, J. (1995). Novel magnetic properties of carbon nanotubes. *Phys. Rev. Lett.*, Vol. 74, No. 7, 1123-1126, ISSN 1079-7114
- Ma, Y.; Lehtinen, P. Foster, A. & Nieminen. (2004). Magnetic properties of vacancies in graphene and single-walled carbon nanotubes. *New J. Phys.*, Vol. 6, No. 1, 68-1-15, ISSN 1367-2630
- Maiti, A.; Svizhenko, A. & Anantram, M. (2002). Electronic transport through carbon nanotubes: effects of structural deformation and tube chirality. *Phys. Rev. Lett.*, Vol. 88, No. 12, 126805-1-4, ISSN 1079-7114
- Mazzoni, M. & Chacham, H. (2000). Bandgap closure of a flattened semiconductor carbon nanotube: a first principal study. *Appl. Phys. Lett.*, Vol. 76, No. 12, 1561-1563, ISSN 0003-6951
- Mehrez, H.; Svizhenko, A.; Anantram, M.; Elstner, M. & Frauenheim, T. (2005). Analysis of band-gap formation in squashed armchair carbon nanotubes. *Phys. Rev. B*, Vol. 71, No. 15, 155421-1-7, ISSN 1098-0121
- Minary-Jolandan, M. & Yu, M.-F. (2008). Reversible radial deformation up to the complete flattening of carbon nanotubes in nanoindentation. *J. Appl. Phys.*, Vol. 103, No. 7, 073516-1-5, ISSN 0021-8979
- Minot, E.; Yaish, Y.; Sazonova, V & McEuen, P. (2004). Determination of electron orbital magnetic moments in carbon nanotubes. *Nature*, Vol. 428, No. 6982, 536-539, ISSN 0028-0836. Figure 6b is used with permission from Macmillan Publisher Ltd: Nature, Copyright 2004.
- Moradian, R. & Azadi, S. (2006). Boron and nitrogen-doped single-walled carbon nanotube. *Physica E*, Vol. 35, No. 1, 157-160, ISSN 1386-9477. Figure 5b is used with permission from Elsevier, Copyright 2005.
- Nakada, K.; Fujita, M.; Dresselhaus, G. & Dresselhaus, M. (1996). Edge states in graphene ribbon: nanometer size effects and edge shape dependence. *Phys. Rev B*, Vol. 54, No. 24, 17954-17961, ISSN 1098-0121
- Nardelli, M.; Fattebert, J.-L.; Orlikowski, D.; Roland, C.; Zhao, Q. & Bernholc, J. (2000). Mechanical properties, defects and electronic behavior of carbon nanotubes. *Carbon*, Vol. 38, No. 11-12, 1703-1711, ISSN 0008-6223

- Neugebauer, J. & Scheffler, M. (1992). Adsorbate-substrate and adsorbate-adsorbate interactions of Na and K adlayers on Al(111). *Phys. Rev. B*, Vol. 46, No. 24, 16067-106080, ISSN 1098-0121
- Nevidomskyy, A.; Csanyi, G. & Payne, M. (2003). Chemically active substitutional nitrogen impurity in carbon nanotubes. *Phys. Rev. Lett.*, Vol. 91, No. 10, 105502-1-4, ISSN 1079-7114
- Orellana, W. & Fuentealba, P. (2006). Structural, electronic and magnetic properties of vacancies in single-walled carbon nanotubes. *Surf. Sci.*, Vol. 600, No. 18, 4305-4309, ISSN 0039-6028
- Park, C.; Kim, Y. & Chang, K. (1999). Band-gap modification by radial deformation in carbon nanotubes. *Phys. Rev. B*, Vol. 60, No. 15, 10656-10659, ISSN 1098-0121
- Picozzi, S.; Santucci, S. & Lozzi, L. (2004). Ozone adsorption on carbon nanotubes: the role of Stone-Wales defects. *J. Chem. Phys.*, Vol. 120, No. 15, 7147-7152, ISSN 0021-9606
- Reich, S.; Thomsen, C. & Maultzsch, J. (2004). Carbon Nanotubes. *EILEY-VCH Verlag GmbH & Co. KGaA*, ISBN 3-527-40386-8
- Rossato, J.; Baierle, R.; Fazzio, A. & Mota, R. (2005). Vacancy formation process in carbon nanotubes: first-principal approach. *Nano Lett.*, Vol. 5, No. 1, 197-200, ISSN 1530-6984
- Santos, E.; Ayuela, A.; Fagan, S.; Filho, J. Azevedo, D.; Souza, A. & Sanchez-Portal, D. (2008). Switching on magnetism in Ni-doped graphene: density functional calculation. *Phys. Rev. B*, Vol. 78, No. 19, 195420-1-5, ISSN 1098-0121
- Shan, B.; Lakatos, G.; Peng, S. & Cho, K. (2005). First-principal study of band-gap change in deformed nanotubes. *Appl. Phys. Lett.*, Vol. 87, No. 17, 173109-1-3, ISSN 0003-6951. Figure 3 is used with permission from American Institute of Physics, Copyright 2005.
- a Shtogun, Y. & Woods, L. (2009). Electronic and magnetic properties of deformed and defective single wall carbon nanotubes. *Carbon*, Vol. 47, No. 14, 3252-3262, ISSN 0008-6223
- b Shtogun, Y. & Woods, L. (2009). Electronic structure modulations of radially deformed single wall carbon nanotubes under transverse external electric fields. *J. Phys. Chem. C*, Vol. 113, No. 12, 4792-4796, ISSN 1932-7447
- Shtogun, Y, Woods, L. & Dovbeshko, G. (2007). Adsorption of adenine and thymine and their radicals on single-wall carbon nanotubes. *J. Phys. Chem. C*, Vol. 111, No. 49, 18174-18181, ISSN 1932-7447
- Son, Y.; Ihm, J.; Cohen, M.; Louie, S. & Choi H. (2005). Electrical switching in metallic carbon nanotubes. *Phys. Rev. Lett.*, Vol. 95, No. 21, 216602-1-4, ISSN 1079-7114
- Stone, A. & Wales, D. (1986). Theoretical studies of icosahedral C₆₀ and some related species. *Chem Phys. Lett.*, Vol. 128, No. 5-6, 501-503, ISSN 0009-2614
- Suenaga, K.; Wakabayashi, H.; Koshino, M.; Sato, Y.; Urita, K. & Iijima, S. (2007). Imaging active topological defects in carbon nanotubes. *Nature Nanotechnology*, Vol. 2, No. 6, 358-360, ISSN 1748-3387
- Sugie, H.; Tanemura, M.; Filip, V.; Iwata, K.; Takahashi, K. & Okuyama, F. (2001). Carbon nanotubes as electron source in an x-ray tube. *Appl. Phys. Lett.*, Vol. 78, No. 17, 2578-2580, ISSN 0003-6951

- Tang, J.; Qin, L.-C.; Sasaki, T.; Yudasaka, M.; Matsushita, A. & Iijima, S. (2000). Compressibility and polygonization of single-wall carbon nanotubes under hydrostatic pressure. *Phys. Rev. Lett.*, Vol. 85, No. 9, 1887-1889, ISSN 1079-7114
- Tans, S.; Verschueren, A. & Dekker, C. (1998). Room-temperature transistor based on a single carbon nanotube. *Nature*, Vol. 393, No. 6680, 49-52, ISSN 0028-0836
- Tien, L.; Tsai, C.; Li, F. & Lee, M. (2005). Band-gap modification of defective carbon nanotubes under a transverse electric field. *Phys. Rev. B*, Vol. 72, No. 24, 245417-1-6, ISSN 1098-0121. Figure 7 is used with permission from American Institute of Physics, Copyright 2005.
- Tien, L.-G.; Tsai, C.-H.; Li, F.-Y. & Lee, M.-H. (2008). Influence of vacancy defect on electronic properties of armchair single wall carbon nanotube. *Diam. Relat. Mater.*, Vol. 17, No. 4-5, 563-566, ISSN 0925-9635
- Tombler, T.; Zhou, C.; Alexseyev, L.; Kong, J.; Dai, H.; Liu, L.; Jayanthi, C.; Tang, M. & Wu, S. (2000). Reversible electromechanical characteristics of carbon nanotubes under local-probe manipulation. *Nature*, Vol. 405, No. 6788, 769-772, ISSN 0028-0836. Figure 1 is used with permission from Macmillan Publisher Ltd: Nature, Copyright 2000.
- Vitali, L.; Burghard, M.; Wahl, P.; Scheider, M. & Kern, K. (2006). Local pressure-induced metallization of a semiconducting carbon nanotube in a crossed junction. *Phys. Rev. Lett.*, Vol. 96, No. 8, 086804-1-4, ISSN 1079-7114
- Vukovic, T.; Milosevic, I. & Damjanovic, M. (2002). Carbon nanotubes band assignment, topology, Bloch states, and selection rules. *Phys. Rev. B*, Vol. 65, No. 4, 045418-1-9, ISSN 1098-0121
- Wang, C.; Zhou, G.; Liu, H.; Wu, J.; Qiu, Y.; Gu, B.-L. & Duan, W. (2006). Chemical functionalization of carbon nanotubes by carboxyl groups on Stone-Wales defects: a density functional theory study. *J. Phys. Chem. B*, Vol. 110, No. 21, 10266-10271, ISSN 1089-5647
- Woods, L.; Badescu, S. & Reinecke, T. (2007). Adsorption of simple benzene derivatives on carbon nanotubes. *Phys. Rev. B*, Vol. 75, No. 15, 155415-1-9, ISSN 1098-0121
- Wu, J. & Hagelberg, F. (2009). Magnetism in finite-sized single-walled carbon nanotubes of zizzag type. *Phys. Rev. B*, Vol. 79, No. 11, 115436-1-9, ISSN 1098-0121
- Yang, S.; Shin, W. & Kang, J. (2006). Ni adsorption on Stone-Wales defect sites in single-wall carbon nanotubes. *J. Chem. Phys.*, Vol. 125, No. 8, 084705-1-5, ISSN 0021-9606
- Yao, Z.; Postma, H.; Balents, L. & Dekker, C. (1999). Carbon nanotube intramolecular junction. *Nature*, Vol. 402, No. 6759, 273-276, ISSN 0028-0836
- Yi, J.-Y. & Bernholc, J. (1993). Atomic structure and doping of microtubules. *Phys. Rev. B*, Vol. 47, No. 3, 1708-1711, ISSN 1098-0121
- Yuan, J. & Liew, K. (2009). Effects of vacancy defect reconstruction on the elastic properties of carbon nanotubes. *Carbon*, Vol. 47, No. 6, 1526-1533, ISSN 0008-6223
- Zhang, J.; Yang, G.; Cheng, Y.; Gao, B.; Qiu, Q. & Lee, Y. (2005). Stationary scanning x-ray source based on carbon nanotube field emitters. *Appl. Phys. Lett.*, Vol. 86, No. 18, 184104-1-3, ISSN 0003-6951
- Zheng, G. & Zhuang, H. (2008). Magneto-mechanical coupling behavior of defective single-walled carbon nanotubes. *Nanotechnology*, Vol. 19, No. 32, 325701-1-9, ISSN 0957-6984



Carbon Nanotubes

Edited by Jose Mauricio Marulanda

ISBN 978-953-307-054-4

Hard cover, 766 pages

Publisher InTech

Published online 01, March, 2010

Published in print edition March, 2010

This book has been outlined as follows: A review on the literature and increasing research interests in the field of carbon nanotubes. Fabrication techniques followed by an analysis on the physical properties of carbon nanotubes. The device physics of implemented carbon nanotubes applications along with proposed models in an effort to describe their behavior in circuits and interconnects. And ultimately, the book pursues a significant amount of work in applications of carbon nanotubes in sensors, nanoparticles and nanostructures, and biotechnology. Readers of this book should have a strong background on physical electronics and semiconductor device physics. Philanthropists and readers with strong background in quantum transport physics and semiconductors materials could definitely benefit from the results presented in the chapters of this book. Especially, those with research interests in the areas of nanoparticles and nanotechnology.

How to reference

In order to correctly reference this scholarly work, feel free to copy and paste the following:

Yaroslav V. Shtogun and Lilia M. Woods (2010). Properties of Carbon Nanotubes under External Factors, Carbon Nanotubes, Jose Mauricio Marulanda (Ed.), ISBN: 978-953-307-054-4, InTech, Available from: <http://www.intechopen.com/books/carbon-nanotubes/properties-of-carbon-nanotubes-under-external-factors>

INTECH
open science | open minds

InTech Europe

University Campus STeP Ri
Slavka Krautzeka 83/A
51000 Rijeka, Croatia
Phone: +385 (51) 770 447
Fax: +385 (51) 686 166
www.intechopen.com

InTech China

Unit 405, Office Block, Hotel Equatorial Shanghai
No.65, Yan An Road (West), Shanghai, 200040, China
中国上海市延安西路65号上海国际贵都大饭店办公楼405单元
Phone: +86-21-62489820
Fax: +86-21-62489821

© 2010 The Author(s). Licensee IntechOpen. This chapter is distributed under the terms of the [Creative Commons Attribution-NonCommercial-ShareAlike-3.0 License](#), which permits use, distribution and reproduction for non-commercial purposes, provided the original is properly cited and derivative works building on this content are distributed under the same license.